# RADIATION HEAT TRANSFER CHARACTERISTICS OF TURBINE VANE AIRFOILS IN A WATER-COOLED CASCADE

by Herbert J. Gladden, Steven A. Hippensteele, Robert O. Hickel, and Robert P. Dengler

Lewis Research Center

## SUMMARY

An analytical and experimental study was made to determine the net radiation heat loss from solid uncooled vanes to water-cooled walls of a cascade. To accomplish this goal, the measured airfoil temperature was compared with a calculated adiabatic airfoil temperature, and the difference then attributed to radiation heat loss. Equations were derived that described the net radiation heat loss.

Experimental studies were made of the thermal characteristics of the vanes for gas temperature levels ranging from about $1460^{\circ}$ to $2060^{\circ}$ R (811 to 1144 K). The investigation was made for a constant midchannel midspan exit Mach number of 0.85 (design Mach number).

The results showed that for the particular vane and cascade geometry investigated, a significant net radiation heat loss from the vanes to the cascade walls existed. The thermal calibration showed that for a cascade operating condition which might be typical of that employed when cooled vanes are being investigated (a combustion gas temperature of $2960^{\circ}$ R (1644 K) and a vane airfoil temperature of $2260^{\circ}$ R (1256 K) at the vane midspan) the temperature correction due to radiation at the leading edge region of the airfoil was about $50^{\circ}$ R (28 K). The correction for the midchord and trailing edge regions was about $70^{\circ}$ R (39 K).

## INTRODUCTION

In turbine cooling studies it is common practice to determine the performance of cooled airfoils by experimental investigations conducted in a cascade facility. Because these facilities may be designed to operate at combustion gas temperatures on the order of $3000^{\circ}$ R (1667 K) or higher, it is necessary to cool the walls and ducting of the

cascade in order to maintain structural soundness and durability. Such cooling is often achieved by the use of water, which can result in cascade gas-side wall-surface-temperatures on the order of $650^{\circ}$ to $850^{\circ}$ R (362 to 472 K). Vane airfoil temperatures, however, might be on the order of $2050^{\circ}$ to $2450^{\circ}$ R (1138 to 1362 K). Therefore, in the case of water cooled cascades, significant amounts of heat may be radiated from the relatively hot airfoil to the cooler cascade walls. For certain research applications it is desirable to know with reasonable accuracy the amount of heat that is radiated to the cooler walls so that a more precise knowledge of the actual cooling performance of the airfoil can be obtained. Because of the rather complicated geometry of cascade ducting and other factors (such as radiation from combustion gases to the airfoil and the emissivity of the surfaces), it is generally not possible to analytically calculate the radiation heat exchange accurately.

This report describes an analytical and experimental study that was made to determine the net radiation heat loss from solid uncooled vanes to water-cooled walls of a cascade facility. A thermal radiation correction technique was evolved that required experimentally determined calibration parameters. The technique involved the measurement of airfoil temperatures that were compared with calculated adiabatic airfoil temperatures; any temperature differences were then attributed to radiation heat loss (or gain).

The correction technique developed is based on a three-dimensional heat balance and a relatively simple experimental calibration process. Although the experimental results presented are applicable only to a given facility, the general approach can be applied to other types of heat-transfer experiments wherein the radiation heat-transfer characteristics are desired but are not amenable to a rigorous analytical solution. The method developed accounts for (1) radiation from the airfoil surfaces to the cooler cascade walls, (2) radiation from the combustion gases to the airfoil surfaces, (3) the geometry of the various airfoil and cascade surfaces involved, and (4) the emissivity of the radiating surfaces.

The radiation correction factors for the cascade in question were determined by experimentally investigating solid, noncooled turbine vanes that were instrumented with an array of thermocouples. The vanes had a span of 4 inches (10.2 cm) and a chord of 2.5 inches (6.4 cm). The investigation was made over a range of combustion gas temperatures from $1460^{\circ}$ to $2060^{\circ}$ R (811 to 1144 K) at combustion gas pressures of 45 and 90 psia (31 and 62 $N/cm^2$). The midchannel midspan exit Mach number was maintained at 0.85 (the design Mach number). The water flow to the cooled cascade walls was varied to determine the effects of the wall temperature on the radiation characteristics of the vanes. The cascade also had provisions to film cool the inner and outer diameter vane platforms; the effect of no film cooling and of maximum film cooling of the vane platforms on the airfoil temperature and radiation correction factors were also investigated.

## DESCRIPTION OF CASCADE

The cascade facility is described in detail in reference 1. Briefly, it consisted of an inlet section, burner section, transition section, test section, and exit section as shown schematically in figure 1. The transition, test, and exit sections were water cooled. A schematic diagram of the test section is shown in figure 2. Four vanes were accommodated in the test section; however, only vanes in positions 2 and 3 (fig. 2) were considered test vanes. The vanes in positions 1 and 4 were considered slave vanes whose primary purposes were to provide suitable flow channels around the test vanes (see ref. 2 for a discussion of the aerodynamic characteristics of the cascade) and to provide surfaces whose temperature level was about the same as the test vanes so that radiation heat transfer from the test vanes to the slave vanes (or vice versa) was minimized. For heat-transfer investigations, the test vanes would be fully instrumented while the slave vanes would be instrumented only sufficiently to permit monitoring of their general operating conditions. The vanes in positions 1 to 4 will be referred to by their position number.

As shown in figure 2, the cascade test section is equipped with three viewing ports. These viewing ports permit observation of the test vane surfaces with optical types of thermal radiation detectors to determine the surface temperatures of the vanes.

The cascade end walls shown in figure 2 as well as the floor and ceiling of the cascade test section and the walls of the viewports were water-cooled. When the cascade is operated throughout its normal range of gas temperature levels (from about $1460^{\circ}$ to $2960^{\circ}$ R (811 to 1644 K)), the gas-side wall temperatures of the water-cooled components will be on the order of $650^{\circ}$ to $850^{\circ}$ R (362 to 472 K). The cooled vane-airfoil-surface temperatures may be on the order of $1860^{\circ}$ to $2260^{\circ}$ R (1033 to 1256 K).

For the calibration tests, four solid uncooled vanes were installed in the cascade test section as indicated in figure 2. The vanes had a span of 4 inches (10.2 cm) and a chord of 2.5 inches (6.3 cm). The external profile of the vane airfoils used were the same as those that are expected to be used in the cascade for cooling performance studies.

### Vane Instrumentation

Vanes 2 and 3 were instrumented with Chromel-Alumel thermocouples that were contained within stainless-steel sheaths having an outside diameter of 0.020 inch (0.051 cm). The thermocouple sheaths were placed in grooves machined into the vane surface and held in place by a series of 0.002-inch (0.005-cm) diameter wires that were spot-welded to the vane walls. After placement of the thermocouples, the remaining slot

around the thermocouple installation was filled with a ceramic cement and hand dressed so that there was a continuous, smoothly faired surface having essentially the same airfoil profile that existed before installation of the thermocouples. The thermocouple junctions were within about 0.010 inch (0.025 cm) of the vane gas-side surface.

Twenty-five thermocouples were installed on the airfoils of vanes 2 and 3 as shown in figure 3. There were 11 thermocouples placed around the periphery of the vane at the midspan plane of the airfoils. Seven thermocouples were placed around the airfoil at a hub plane 0.64 inch (1.63 cm) from the inner diameter platform and 7 thermocouples were placed around the airfoil at a tip plane 0.64 inch (1.63 cm) from the outer diameter platform. These positions are hereinafter referred to as the hub and tip thermocouple locations, respectively. Figure 4 shows the suction surface of vanes 2 and 3 after the thermocouple instrumentation has been completely installed in the airfoils.

## Cascade Gas-Side-Wall Instrumentation

Because of the double-wall water-cooled design of the cascade in the region of the test section, it was not practical to provide extensive temperature instrumentation of the gas-side surface of the inner wall. Furthermore, it was believed that the water-cooled walls would cool uniformly and that there would not be large local temperature variations in the inner wall temperature and, therefore, no need for numerous temperature measurements. In order to obtain an indication of the temperature level of the inner walls, a thermocouple was installed in each end wall of the test section about 1 inch (2.54 cm) upstream of the vane leading edge plane. The inner wall was about 0.12 inch (0.32 cm) thick with approximately 0.02 inch (0.05 cm) of ceramic coating on the hot side. The thermocouples were placed on the water-side surface of the inner wall.

## General Facility Instrumentation

The cascade facility was equipped with general operational instrumentation to permit measuring the temperature and pressure of the water, fuel, air, and combustion gas being supplied to the facility. Flow quantities of the fuel, water, combustion gas, and air were measured by flowmeters. The details of the general instrumentation and the automatic data acquisition system for the facility are given in reference 1. As shown in figure 2 the inlet gas conditions were measured in front of channels 2 to 4. Radially traversing probes were located in front of channels 3 and 4, and consisted of a total tem-

perature probe and a total pressure probe, respectively. The static pressure was measured at the inner diameter platform only.

## DERIVATION OF THE RADIATION CORRECTION FACTOR, CALIBRATION PARAMETER, AND EFFECTIVE GAS TEMPERATURE

A radiation correction factor and an associated calibration parameter were derived by applying a simple heat balance to an isolated element of a test vane airfoil. This heat balance was first applied to a case where no heat was lost by radiation to the surroundings and then a similar case was considered which included radiation heat loss. For this analysis it was assumed that the products of combustion formed a nonluminous gas and that the contribution to the heat input to the vanes by the flame and nonluminous gas was negligible.

### Case I - Vane Cooling with no Radiation Heat Loss

A unit volume element of a turbine vane is shown schematically in figure 5(a); the vane was assumed to be cooled internally and to have no heat-loss due to radiation. From a heat balance

$$q_{o,I} = q_{i,I} + \sum q_{k,I} = (T_{ge} - T_{wo})h_o \tag{1}$$

Also

$$\frac{1}{2}\sum q_{k,I}\left(\frac{t}{k}\right) + q_{i,I}(R) = T_{wo} - T_c \tag{2}$$

where $R = t_w/k_w + 1/h_c$ and is the resistance coefficient. (See appendix A for the definition of the symbols used herein.) Adding equations (1) and (2) yields the following definition of temperature difference between the effective gas temperature and the coolant temperature:

$$\frac{q_{i,I}}{h_o} + q_{i,I}(R) + \sum q_{k,I}\left(\frac{1}{h_o} + \frac{t}{2k}\right) = T_{ge} - T_c \tag{3}$$

## Case II - Vane Cooling with Radiation Heat Loss

If there is significant thermal radiation from the vane airfoil surface to the cascade walls and conduction in the spanwise and chordwise directions during operation of the cascade, the measured vane airfoil temperatures will be less than that which would exist under case I conditions. In order to accurately determine the actual cooling performance of a given internal cooling configuration, the measured temperatures must be corrected to compensate for the heat loss.

Figure 5(b) shows a unit volume element of a vane airfoil where radiation from the gas-side surface to a heat sink is encountered. For this case the measured gas-side airfoil temperature $T_{wm}$ is different from the gas-side airfoil temperature that would be observed without heat loss $T_{wo}$. Specifically, $T_{wm}$ is less than $T_{wo}$ because of the heat radiated from the airfoil surface to the relatively cool test section walls. The validity of the previous statement assumes that $h_o$ and $T_{ge}$ are the same in cases I and II. This implies that the gas stream supplies more heat to the vane through a greater temperature difference when radiated heat loss is involved.

If the same type of heat balance is applied in case II as was applied in case I, the following equations are obtained:

$$\frac{q_{o,II}}{h_o} = \frac{q_{i,II}}{h_o} + \frac{\sum q_{k,II}}{h_o} + \frac{q_r}{h_o} = T_{ge} - T_{wm} \tag{4}$$

$$\frac{1}{2}\sum q_{k,II}\left(\frac{t}{k}\right) + q_{i,II}(R) = T_{wm} - T_c \tag{5}$$

Subtracting equation (5) from equation (2),

$$\frac{t}{2k}\left(\sum q_{k,I} - \sum q_{k,II}\right) + (q_i - q_{i,II})R = T_{wo} - T_{wm} \tag{6}$$

Also, subtracting equation (1) from equation (4) results in

$$\frac{(q_{i,II} - q_{i,I})R}{R} + \left(\sum q_{k,II} - \sum q_{k,I}\right) + q_r = (T_{wo} - T_{wm})h_o \tag{7}$$

Substituting equation (6) into equation (7) and rearranging results in a definition for a corrected measured airfoil temperature

$$T_{w,corr} = T_{wo} = T_{wm} + \frac{q_r + \left[\sum q_{k,II} - \sum q_{k,I}\right]\left(\frac{t}{2kR} + 1\right)}{\frac{1}{R} + h_o} \tag{8}$$

The last term on the right will be referred to as the radiation correction factor. It can also be shown that

$$\frac{1}{R} = \frac{h_o(T_{ge} - T_{wm}) - \left(q_r + \sum q_{k,II}\right)}{T_{wm} - T_c - \frac{1}{2}\sum q_{k,II}\left(\frac{t}{k}\right)} \tag{9}$$

and finally that

$$Z' = \frac{\left\{q_r + \left[\sum q_{k,II} - \sum q_{k,I}\right]\left(\frac{t}{2kR} + 1\right)\right\}\left\{T_{wm} - T_c - \frac{1}{2}\sum q_{k,II}\left(\frac{t}{k}\right)\right\}}{h_o(T_{ge} - T_c) - \left(q_r + \sum q_{k,II}\right) - \frac{1}{2}\sum q_{k,II}\left(\frac{th_o}{k}\right)} \tag{10}$$

By assuming that the heat conduction remains unchanged between cases I and II and that the term $\frac{1}{2}\sum q_{k,II}\left(\frac{t}{k}\right)$ is negligible, the radiation correction factor can be reduced to

$$Z = \frac{T_{wm} - T_c}{\frac{h_o}{q_r}(T_{ge} - T_c) - \left(\frac{q_r + \sum q_{k,II}}{q_r}\right)} \tag{10a}$$

The term $q_r + \sum q_{k,II}$ will be referred to as the calibration parameter. The method for determining this parameter is presented in the next section.

## Determination of the Calibration Parameter

The calibration parameter $q_r + \sum q_{k,II}$ was determined experimentally by the procedure described herein. A set of solid vanes (no internal cooling) was installed in the cascade. These vanes were instrumented with a suitable array of thermocouples so that local vane airfoil temperatures could be measured. If conduction and radiation heat loss were not present then the vane surface temperature could be calculated since for

adiabatic members the temperature of the solid member would equal the adiabatic wall temperature. Therefore, the calibration parameter was defined as the difference between the adiabatic airfoil temperature and the measured airfoil temperature (the adiabatic airfoil temperature is referred to here as the effective gas temperature). Therefore,

$$q_r + \sum q_{k,II} \equiv h_o\left[T_{ge} - T_{wm}\right] = \sigma F\left(T_{wm}^4 - T_s^4\right) \tag{11}$$

Also

$$\frac{q_r}{h_o} = T_{ge} - T_{wm} - \frac{\sum q_{k,II}}{h_o} \tag{11a}$$

By inspection of equation (10a) it is noted that the radiation correction factor requires both the heat loss by radiation and the calibration parameter, $q_r + \sum q_{k,II}$. The heat loss by radiation can be determined from the calibration parameter by subtracting the heat conduction terms in three dimensions (span, chord, and transverse). The conduction terms are defined as the temperature gradient at the local airfoil point of interest multiplied by a unit element of area and the ratio of $k_w/h_o$.

The gas-side heat transfer coefficient $h_o$ is calculated at that point of interest using a standard "flat plate" equation for the entire airfoil except the leading edge. A cylinder solution is used for the leading edge (up to $80^o$ from either side of the stagnation point). An average of thermal conductivity $\bar{k}_w$ can be used for the airfoil material.

All of the terms used in the previous equation are measured values or are defined as a function of measured values and a calculated effective gas temperature $T_{ge}$. The local value of the effective gas temperature is dependent on gas conditions around the airfoil.

## Effective Gas Temperature Calculation

The local effective gas temperature $T_{ge}$ was calculated in channel 3 (fig. 2) from the inlet total temperature, the velocity distribution around the vane and a turbulent flow recovery factor. The following equation was used:

$$T_{ge} = T'_{g,i} - (1 - \Lambda)\frac{V^2}{2g_c J C_p} \tag{12}$$

where $\Lambda \equiv Pr_g^{0.333}$ is the recovery factor (ref. 3).

## EXPERIMENTAL PROCEDURE

The objective of the experimental investigation was to obtain the radiation heat transfer characteristics of vanes 2 and 3 in the test section of the cascade for a reasonably wide range of cascade operational variables. Because the vanes were not cooled, extremely high gas temperatures were not included in the test program; the maximum average gas temperature with these vanes was set conservatively at $2060^{\circ}$ R (1145 K). Four nominal gas temperature levels, namely $1460^{\circ}$, $1660^{\circ}$, $1860^{\circ}$, and $2060^{\circ}$ R (811, 922, 1033, and 1144 K) were selected for study of the vane radiation characteristics. A design midspan exit Mach number of 0.85 was used throughout testing. In order to determine whether the temperature of the water-cooled walls varied markedly with coolant flow rate (and in turn effected a significant change in the radiant heat transfer of the vanes) investigations were made with a normal water flow rate through the cascade of 20 gallons per minute (0.0757 $m^3$/min) and a reduced cooling water flow rate of 10 gallons per minute (0.0379 $m^3$/min). To evaluate the effects of the gas stream pressure level, two levels of total pressure entering the cascade test section, namely, 45 and 90 psia (31 and 62 $N/cm^2$), were investigated.

Because of the manner in which the vane platforms were cooled in the cascade test section, an additional variable was investigated. The cascade test section provided for the film cooling (with air) of the inner and outer diameter vane platforms. This film cooling air was directed over the vane platforms from a series of radial slots that were provided in the vane assembly in a plane immediately upstream of the extreme leading edge of the vanes. These slots provide radial injection of film cooling air across the gas channel from end wall to end wall. Because this air was ejected normal to the hot gas stream, it was possible that some of the film cooling air penetrated the hot gas to such a degree that the airfoil temperatures in the hub and tip region of the test airfoils were affected. If the hub and tip region temperatures were appreciably reduced by the film cooling air, heat may be conducted from the midspan region of the airfoil to the cooler hub and tip regions in such quantities that significant reductions in the midspan temperatures may result. The effect of the platform film cooling on airfoil temperatures was investigated by making several tests wherein the maximum amount of film cooling and no film cooling was applied to the vane platforms. Table I contains a listing of the variables by a group number.

## RESULTS AND DISCUSSION

The major part of the investigation was done for the midspan because this was the area least affected by end conditions. However, some results are also presented for

the hub and tip. The experimental results consist of the basic data, calibration parameters for the different areas of the vane airfoil, and finally a study of the effect of heat conduction on the calibration parameters.

The basic data consist of the metal temperatures of the two test vanes and the local calculated effective gas temperature associated with each thermocouple position as determined from equation (12).

## Airfoil Temperature Distributions

Initially the experimental vane airfoil temperature distributions for both test vanes were plotted for the range of gas temperatures studied, at design Mach number, and without film cooling on the platforms. Sample profiles are shown in figure 6 for the tip, midspan, and hub. The measured vane metal temperature $T_{wm}$ is plotted on the ordinate and the abscissa is a dimensionless surface distance $d/L$ from the leading edge. Each set of curves represents midspan nominal inlet total gas temperature levels of $1460^{\circ}$, $1660^{\circ}$, $1860^{\circ}$, and $2060^{\circ}$ R (811, 922, 1034, and 1144 K).

It can be seen that vane 2 generally operated up to $40^{\circ}$ R (22 K) hotter than vane 3 for the range of gas temperatures investigated. This variation was probably caused by variations in the gas stream temperature profile in the transverse direction. The gas stream spanwise temperature profile was obtained only immediately upstream of channel 3. The exact gas temperature level entering channels 2 and 4 was not known but was assumed the same as that for channel 3.

The chordwise temperature patterns shown in figure 6 are typical of the airfoil temperatures for all test conditions. It can be seen that the leading-edge region generally was on the order of $25^{\circ}$ R (14 K) hotter than the midchord or trailing edge regions of the airfoils. There were minor differences in the temperatures of the suction and pressure sides of the airfoils at a given chordwise location.

## Comparison of Measured and Calculated Airfoil Temperatures

By assuming the vane airfoil to be an adiabatic member (case I), the local vane airfoil temperatures could be calculated from gas conditions as discussed previously. Comparison of these calculated temperatures and the measured local temperatures provided an indication of the actual heat gain or loss from the vane surface. This comparison of data is shown in figure 7 where the calculated local effective gas temperature

$T_{ge}$ is plotted on the ordinate and the local measured airfoil temperature $T_{wm}$ is plotted on the abscissa for all thermocouple locations. The midspan data are shown in figures 7(a) and (b) and are representative of all conditions investigated such as temperature and pressure level, sink temperature, and the amount of film cooling applied at the vane platforms. The hub and tip data are shown in figure 7(c) for the case of no film cooling of the vane platforms.

Radiation heat loss at vane midspan without platform cooling. - Figure 7(a) shows data for the midspan without film cooling of the platforms. If the vanes were true adiabatic members, the data points in figure 7(a) would lie on a $45^{\circ}$ line which is represented by the solid line in the figure. It can be seen, however, that the data points lie to the left of the solid line which indicates the measured airfoil temperatures were lower than the calculated values and that there was heat loss from the airfoil. A dashed line has been drawn through the data of figure 7(a), and it can be seen that this line diverges from the solid line as the temperature increases. This indicates that increasing heat loss occurred from the vanes as the temperature level of the vanes increased. These results also suggest that heat loss from the vane airfoil to the cooler cascade walls was through radiation heat transfer since conduction losses would remain nearly constant with increasing temperature level because the temperature gradient in the conduction equation does not change significantly. If the heat sink (cascade walls) remains at approximately the same temperature level (as was the case), the radiation heat losses from the airfoil would be expected to increase as the airfoil temperature increased.

Radiation heat loss at vane midspan with platform film cooling. - In figure 7(b) the midspan temperatures were plotted for the case where the vane platforms were film cooled. The dashed line in figure 7(b) represents the data of figure 7(a) (no platform cooling). It can be seen in figure 7(b) that the data obtained with platform cooling generally lie to the left of the dashed line; this indicates that platform cooling further decreased the temperature of the midspan compared with the case of no platform cooling. The additional temperature reduction was the result of heat loss by conduction from the airfoil midspan to the cooler hub and tip regions of the vane that result when cooling of the vane platforms was employed. It appears that even though the vane platforms are 2 inches (5.1 cm) from the midspan, the cooling of these platforms did reduce the temperature of the midspan on the order of $5^{\circ}$ to $25^{\circ}$ R (3 to 14 K).

Radiation heat loss at vane hub and tip without platform film cooling. - Figure 7(c) shows data for the hub and tip of the airfoil for the case of no platform film cooling. The dashed line drawn through the data points represents an approximate average line, through the data. The data for both the hub and tip show the same trends that have previously been discussed for the midspan. The hub and tip results are very similar to

that obtained for the midspan in that the experimentally obtained metal temperatures were generally on the order of $25^{\circ}$ to $50^{\circ}$ R (14 to 28 K) less than the calculated temperatures.

No attempt was made to make an in-depth study of the radiation heat loss when the vane platforms were film cooled. Limited experimental data obtained in the hub and tip regions with platform film cooling indicated the film cooling jets penetrated radially into the gas stream a significant distance. The mixing of the film cooling air with the combustion gas in the vicinity of the vane platforms reduced the temperature of the combustion gas near the inner and outer diameter platforms. This mixing was initiated immediately upstream of the vane leading-edge plane and downstream of the instrumentation plane in which the combustion gas temperatures were measured. Therefore, the actual combustion gas temperature effecting heat transfered into the vane airfoil at the planes in which the hub and tip airfoil temperatures were measured was not known. This then precluded the possibility of accurately calculating the local effective gas temperature (local adiabatic vane metal temperatures) for the hub and tip.

## Calibration Parameter

With the experimental data obtained, it was possible to calculate the calibration parameter defined previously (see eq. (11)) and in turn to determine the radiation correction factors as defined by equation (10a). Theoretically, a calibration parameter and associated radiation correction factor existed for each location on the vane airfoil surface. Furthermore, each operating variable in the experiment (in this case, the cascade) can possibly effect the radiation characteristics of the surface location under consideration.

Inspection of the airfoil temperature data such as that shown in figures 6 and 7 indicated that the local surface temperatures for a given spanwise plane could be grouped according to position on the airfoil; that is, the leading edge thermocouples were at one general temperature level, the midchord thermocouples at a slightly lower level, and the trailing edge thermocouples at a still lower level. For example, when considering the midspan temperatures, thermocouples 1, 2, and 11 (see fig. 3) were considered as representative of the leading edge, thermocouples 3 and 10 were considered as a pair typical of temperatures aft of the leading edge to about the 50 percent chord position, and, finally, thermocouples 4 to 9 were considered a group typical of the aft 50 percent of the airfoil including the trailing edge region. These groupings of thermocouples (and their respective temperature data) will be referred to as leading edge, midchord, or trailing edge thermocouples or temperatures. Table II summarizes the thermocouple locations considered within each of the spanwise planes that were instrumented. The

calibration parameters and the radiation correction factors were determined for each of the generalized groups.

The calibration parameter $q_r + \sum q_{k,II}$ was defined in equation (11) as being equal to $h_o(T_{ge} - T_{wm})$. Equation (11) also indicated that the calibration parameter was a function of the difference of $T_{wm}$ to the fourth power and $T_s$ to the fourth power. The experimental results obtained indicated that the cascade gas side wall temperature $T_s$ remained nearly constant at a value of about $660^\circ$ R (367 K) for all test conditions. Because $660^4$ is a relatively small number compared with values of the airfoil temperature $T_{wm}$ to the fourth power, the $T_s$ term in equation (11) was dropped. As a consequence, the results presented considered the calibration parameter $q_r + \sum q_{k,II}$ to be a function only of $T_{wm}$.

The average calibration parameters for the midspan plane of vanes 2 and 3 are plotted in figure 8 as a function of the vane airfoil temperature $T_{wm}$. The data are presented for the leading edge, midchord, and trailing edge regions for conditions of no platform cooling and platform cooling. A curve representing a best fit of the plotted data was placed on each figure.

It can be seen that there was a fairly large scatter of the data for each condition illustrated in figure 8. This scatter is to be expected when one considers that the actual thermocouple data probably had an error of the order of ±1 percent. This would result in a temperature uncertainty of $\pm 10^\circ$ R (6 K) for the lowest airfoil temperature regime and about $\pm 16^\circ$ R (9 K) for the highest airfoil temperatures. In general, the data point scatter in figure 8 is no greater than ±4000 Btu per hour per square foot (4545 J/(hr)($cm^2$)) from the curves drawn through the data. Some of the data scatter in figure 8 may also be attributed to error in measuring gas temperature which in turn was introduced into the calculation of the local effective gas temperature. The effects of this data scatter on the radiation correction factor will be indicated in appendix B. The results shown in figure 8 indicate that for the airfoil temperature investigated, the value of the calibration parameter ranged from a minimum of about 4000 (4545) to a maximum of about 18 000 Btu per hour per square foot (20 450 J/(hr)($cm^2$)). The data further indicate that as would be expected, the value of the calibration parameter for a given region increased as the general level of the airfoil temperature increased. Comparison of the values of the calibration parameter for each of the general regions indicated that the leading edge values were about 16 to 40 percent lower than those for the midchord and trailing edge regions. It might be expected that, since the leading edge region was hotter than the midchord or trailing edge regions for a given operating condition, the calibration parameter would be highest for the leading edge. The fact that it was lower suggested that the leading edge was subjected to a lower net radiant energy loss than the

other regions; or more specifically, the leading edge was subjected to a significant gain in radiant energy. The source for such radiant energy was the flame and the nonluminous gases that could be "seen" readily by the vane leading edges.

It can also be seen from figure 8 that the use of film cooling air to cool the vane platforms resulted in an increase in the value of the calibration parameter. For example, if figures 8(a) and (b) are compared, it can be seen that the average value of the calibration parameter for vanes having film cooled platforms (fig. 8(b)) was about 1000 Btu per hour per square foot (1136 J/(hr)($cm^2$)) higher than that for the case of no film cooling (fig. 8(a)). Similar results can be observed for the midchord (figs. 8(c) and (d)) and the trailing edge (figs. 8(e) and (f)). For the midchord and trailing edge regions the platform cooling air had a greater effect than for the leading edge with the calibration parameter values being about 2000 Btu per hour per square foot (2272 J/(hr)($cm^2$)) greater with platform cooling than for the case of no platform cooling. Hence, platform film cooling has increased the conductive cooling component of the resulting calibration parameter. Also, because the cascade gas side wall temperature $T_s$ did not vary significantly between the maximum and minimum coolant water flow conditions, the value of the calibration parameter was not significantly affected as shown in figures 8(a) to (c).

The values of the calibration parameter for the hub and tip regions of the vanes are shown in figure 9 for the range of vane airfoil temperatures investigated and for the case of no platform cooling. No results for the case of platform cooling are shown because of the uncertainties in determining the gas temperature levels for the hub and tip regions.

The results shown in figures 9(a) to (c) indicate that the calibration parameter values and general trends for the hub and tip regions were similar to those previously obtained for the midspan without platform cooling (figs. 8(a), (c), and (e)).

## Conduction Heat Transfer Term

Modification of the calibration parameter for heat flow due to conduction within the airfoil is described next. Equation (11) defines the calibration parameter with a correction for conduction effects. Fundamentally, the modification for conduction consisted of summing the heat conduction terms in three dimensions (span, chord, and transverse (from the pressure surface to the suction surface)). The local temperature gradients (spanwise, chordwise, and transverse) were found by plotting the vane local airfoil temperatures in the manner shown in figures 10 and 11. Two nominal midspan gas temperatures were selected for the plots, namely, $1460^{\circ}$ and $2060^{\circ}$ R (877 and 1144 K). The data were obtained with platform cooling. The resulting spanwise temperature profiles are shown in figure 10; the leading edge temperatures were plotted as one curve for each

gas temperature level. Because the trailing edge and midchord temperatures were essentially the same, only a single curve was drawn to represent these temperatures. It can be seen that the peak of the curves was shifted to hub-side of the midspan location. This was consistant with the inlet gas temperature profile. The chordwise temperature profiles are shown in figure 11 for the pressure and suction surfaces of the vanes for each gas temperature level. Figure 10 was used to obtain the radial temperature gradients, and figure 11 was used to obtain the chordwise and transverse temperature gradients.

The sum of these thermal gradient terms represented the heat exchanged by conduction. The maximum value of heat loss due to conduction was approximately 4800 Btu per hour per square foot (5455 J/(hr)($cm^2$)) at the leading edge for the high gas temperature level, and the lower temperature level had a conduction loss of approximately 3600 Btu per hour per square foot (4090 J/(hr)($cm^2$)). These values decreased steadily for positions away from the leading edge until at the trailing edge the correction amounted to approximately 2700 and 1700 Btu per hour per square foot (3070 and 1932 J/(hr)($cm^2$)) for gas temperatures of $2060^{\circ}$ and $1460^{\circ}$ R (811 and 1144 K), respectively. The resulting heat conduction term can then be subtracted from the calibration parameter to obtain the radiation heat loss $q_r$.

## Application of Results

The results obtained and presented in this report are intended to be applied to air-cooled vanes installed in the cascade facility. It is expected that for most of the cooled vane investigations the combustion gas temperature will be above the values used herein with noncooled vanes. Because the radiation correction for heat exchange between the vanes under consideration is primarily a function of the level of the vane airfoil temperature and the cascade wall temperature, the calibrations evolved should be applicable providing the cooled vane airfoil temperatures are at about the same temperature levels investigated for the uncooled vanes. Some error in the calibration parameter is to be expected for gas temperatures above those investigated because as the gas temperature increases, there is more radiant heat transfer from the nonluminous combustion gases to the vane surfaces. This effect would be most pronounced at the leading edge region of the vane and would result in a smaller correction at the leading edge than determined from these calibrations. Also, the cascade wall temperature will probably increase with an increase in gas temperature level. However, this wall temperature is not expected to exceed $860^{\circ}$ R (477 K) under the normal operating conditions of the cascade ($2960^{\circ}$ R (1644 K)). A hypothetical numerical example is presented in appendix B to indicate how the results would be applied to an actual cooled vane investigation.

## SUMMARY OF RESULTS

An analytical and experimental study was made to determine the radiation heat loss from test vane airfoils to the relatively cool walls of a water cooled cascade test facility. The study produced the following results:

1. Relatively simple equations were derived from heat-transfer theory that described the net heat loss from the test vane airfoils to the water-cooled cascade walls.

2. The equations made use of a "calibration parameter" and a radiation correction factor to determine the temperature loss. The calibration parameter was determined experimentally from relatively simple tests performed in the cascade in question. The necessary input for the equations involved easily obtained experimental temperatures or readily calculable temperatures that were dependent on the cascade operating conditions and/or the vane gas passage geometry.

3. The experimental results showed that, for the cascade and vane geometry investigated, a net heat loss from the vanes to the cascade walls resulted. Generally, the radiation heat losses from the vanes were appreciable, particularly for vane airfoil temperature levels that are of interest for present day materials, that is, of the order of $2260^{\circ}$ R (1256 K). For this airfoil temperature and for a gas temperature of $2960^{\circ}$ R (1644 K) the temperature correction due to radiation at the midspan leading edge region of the vane was about $50^{\circ}$ R (28 K); for the midchord and trailing edge regions the correction was about $70^{\circ}$ R (39 K).

4. The results obtained suggest that only the midspan of the airfoil should be considered as the test section for sophisticated heat transfer analyses applied to aircooled vanes investigated in the cascade.

Lewis Research Center,
National Aeronautics and Space Administration,
Cleveland, Ohio, November 3, 1970,
720-03.

## APPENDIX A

## SYMBOLS

| | |
|---|---|
| $c_p$ | specific heat |
| d | surface distance from leading edge stagnation point |
| F | configuration factor |
| $g_c$ | gravitation constant |
| h | surface heat-transfer coefficient |
| J | heat equivalent of work |
| k | thermal conductivity |
| L | surface distance from leading edge to trailing edge for either suction or pressure surface |
| $\ell$ | length |
| Pr | Prandtl number |
| q | heat flux per unit area |
| R | resistance coefficient |
| T | temperature |
| t | thickness |
| V | local velocity |
| Z | radiation correction factor |
| $\sigma$ | Stefan-Boltzmann constant |
| $\Lambda$ | recovery factor |

Subscripts:

| | |
|---|---|
| c | coolant |
| corr | corrected |
| e | effective |
| g | gas |
| i | inside (or coolant side) |
| k | conduction |

| | |
|---|---|
| m | measured |
| o | outside (or gas side) |
| r | radiation |
| s | sink |
| w | airfoil |
| I | case I |
| II | case II |

Superscript:

| | |
|---|---|
| ' | total |

## APPENDIX B

## NUMERICAL EXAMPLE

To demonstrate the application of the radiation correction results obtained, the following conditions were assumed to exist during a heat-transfer investigation of an air-cooled vane. This example neglects the conduction effects contained in the calibration parameter and assumes that all the heat loss is by radiation. Upper and lower limits are included with the calibration parameter and the correction factor to indicate the effect of the data scatter.

Combustion gas total temperature at vane midspan, $^{o}R$ (K) . . . . . 2960 (1644)
Combustion gas total pressure, psia ($N/cm^2$) . . . . . 45 (31)
Measured vane metal temperature at leading edge, $^{o}R$ (K) . . . . . 2260 (1256)
Cooling air temperature, $^{o}R$ (K) . . . . . .1460 (811)
Calculated effective gas temperature at leading edge, $^{o}R$ (K) . . . . . 2960 (1644)

To determine the calibration parameter $q_r + \sum q_{k,II}$ and the radiation correction factor Z for the previous conditions, the following procedure is applied:

(1) For the leading edge region midspan position, the value of $q_r + \sum q_{k,II}$ (fig. 8(b)) is found to be 26 000 Btu per hour per square foot (29 540 $J/(hr)(cm^2)$) with a 1000 Btu per hour per square foot (1136 $J/(hr)(cm^2)$) scatter for a vane airfoil temperature of $2260^{o}$ R (1256 K).

(2) The value of Z is determined from equation (10a) and the use of the values of $q_r + \sum q_{k,II}$, $h_o$ (300 $Btu/(hr)(ft^2)(^{o}R)$ (1705 $J/(sec)(m^2)(K)$), $T_{wm}$ ($2260^{o}$ R (1256 K)), $T_c$ ($1460^{o}$ R (811 K)) and $T_{ge}$ ($2960^{o}$ R (1256 K)). It is also assumed that $\left(q_r + \sum q_{k,II}\right)/q_r = 1$. For these conditions $Z = 49.2^{o}\ ^{+6.2^{o}}_{-5.9^{o}}$ R ($27.3\ ^{+3.4}_{-3.3}$ K).

(3) The corrected measured airfoil temperature is then determined from equation (8) and found to be $2309^{o}$ R (1283 K).

If conduction effects due to film cooling the vane platforms and nonuniformity of the effective gas temperature are considered, then the following results are obtained.

(4) From figure 8(b), $q_r + \sum q_{k,II}$ = 26 000 Btu per hour per square foot (29 540 $J/(hr)(cm^2)$).

(5) The heat conduction term can be determined from the known temperature distribution in the vane and a suitable three-dimensional conduction analysis. By assuming the conduction losses in these tests to be similar to that of cooled vane tests, the conduction term was found to be approximately 5000 Btu per hour per square foot (5680 $J/(hr)(cm^2)$). Consequently, the corrected value due to platform cooling and leading edge conduction effects is 21 000 Btu per hour per square foot (23 880 $J/(hr)(cm^2)$).

(6) The value of Z is obtained from equation (10a) and is found to be $43.2^{\circ}$ R (24 K).

(7) The corrected measured leading edge temperature considering the effects of film cooling the vane platforms and conduction effects caused by nonuniform effective gas temperature is, from equation 8, equal to $2303^{\circ}$ R (1280 K).

It can be seen that considering the overall thermal conduction effects decreases the corrected airfoil temperature only $6^{\circ}$ R (3.3 K): from $2309^{\circ}$ R (1283 K) to $2303^{\circ}$ R (1280 K).

Similar calculations can also be made for the midchord and trailing edge regions of the airfoil. Although not shown, the radiation correction factor for the same temperature conditions assumed previously would be of the order of $70^{\circ}$ R (39 K) for the midchord and trailing edge regions. Correcting for thermal conductivity effects results in only a change of about $5^{\circ}$ R (2.8 K) for either location.

It is obvious that the temperatures at the hub and tip region can be corrected in a manner similar to that applied to the midspan position. It should be pointed out, however, that, as indicated previously, the hub and tip wall temperatures are influenced to a greater degree than the midspan temperatures when film cooling is applied to the vane platforms. Furthermore, the effect of film cooling air on the local effective gas temperature was not determined. As a consequence, it was not possible to evaluate thoroughly the effect of conduction on the hub and tip temperatures. The results obtained suggest that only the midspan of the airfoil should be considered as a test section for sophisticated heat-transfer analyses applied to aircooled vanes investigated in the cascade.

## REFERENCES


1. Calvert, Howard F.; Cochran, Reeves P.; Dengler, Robert P.; Hickel, Robert O.; and Norris, James W.: Turbine Cooling Research Facility. NASA TM X-1927, 1970.

2. Gladden, Herbert J.; Dengler, Robert P.; Evans, David G.; and Hippensteele, Steven A.: Aerodynamic Investigation of Four-Vane Cascade Designed for Turbine Cooling Studies. NASA TM X-1954, 1970.

3. Rohsenow, Warren M.; and Choi, Harry Y.: Heat, Mass, and Momentum Transfer. Prentice-Hall, Inc., 1961.


TABLE I. - DATA GROUPS AND VARIABLES CONSIDERED IN EACH GROUP

[Gas stream exit Mach number, 0.85; gas stream temperatures, 1460°, 1660°, 1860°, and 2060° R (811, 922, 1033, and 1144 K.]

| Group | Coolant water flow rate | Platform film cooling | Gas stream pressure | |
|---|---|---|---|---|
| | | | psia | $N/cm^2$ |
| 1 | Minimum | Yes | 45 and 90 | 31 and 62 |
| 2 | Minimum | No | 45 | 31 |
| 3 | Maximum | Yes | 45 and 90 | 31 and 62 |
| 4 | Maximum | No | 45 and 90 | 31 and 62 |

TABLE II. - GROUPING OF THERMOCOUPLES ACCORDING TO GENERALIZED CHORDWISE LOCATIONS

| Generalized chordwise location | Grouping of thermocouples[a] | | |
|---|---|---|---|
| | Hub section | Mean radius section | Tip section |
| Leading edge | 19, 25 | 1, 2, 11 | 12, 13 |
| Midchord | 20, 24 | 3, 10 | 14, 18 |
| Trailing edge | 21, 22, 23 | 4, 5, 6, 7, 8, 9 | 15, 16, 17 |

[a]Thermocouples are identified by their locations as shown in figure 3.

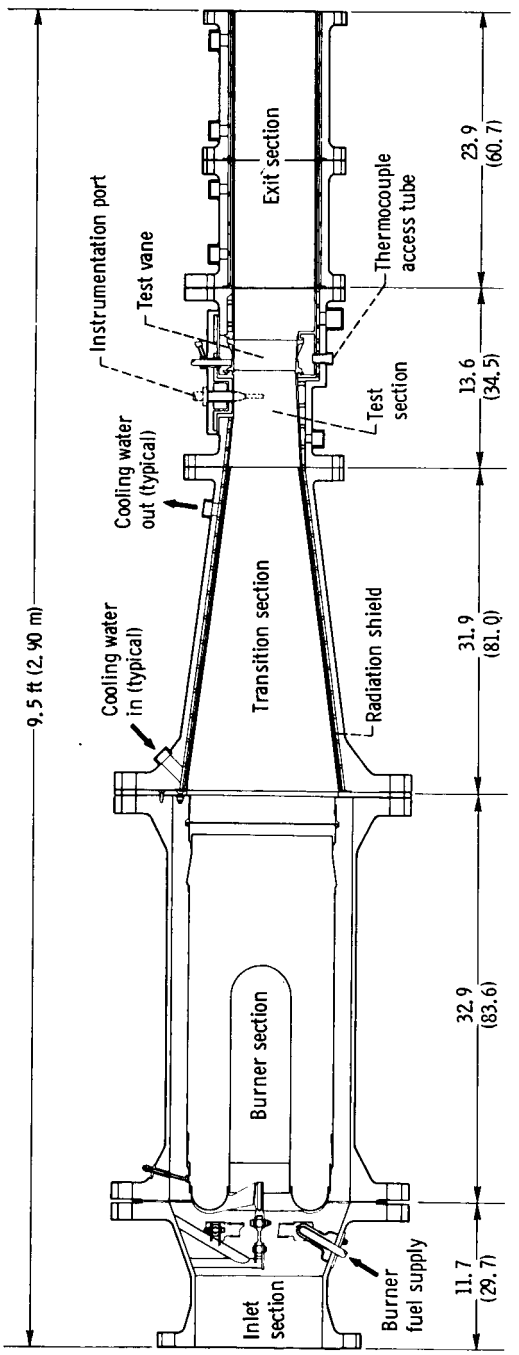


Figure 1. - Schematic cross sectional view of cascade facility. All dimensions are in inches (cm) except where noted.

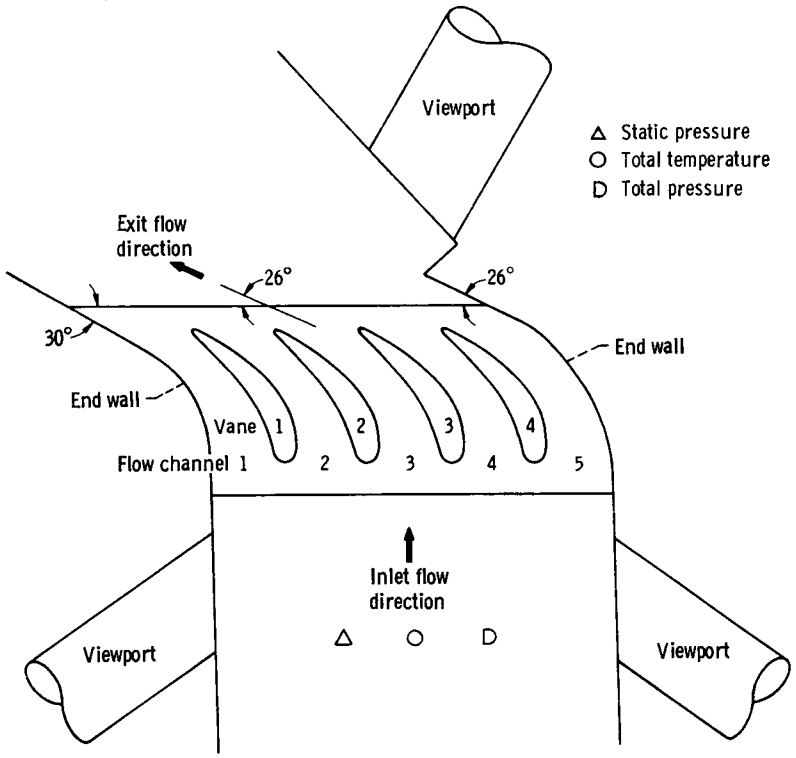


Figure 2. - Schematic view of vane test section.

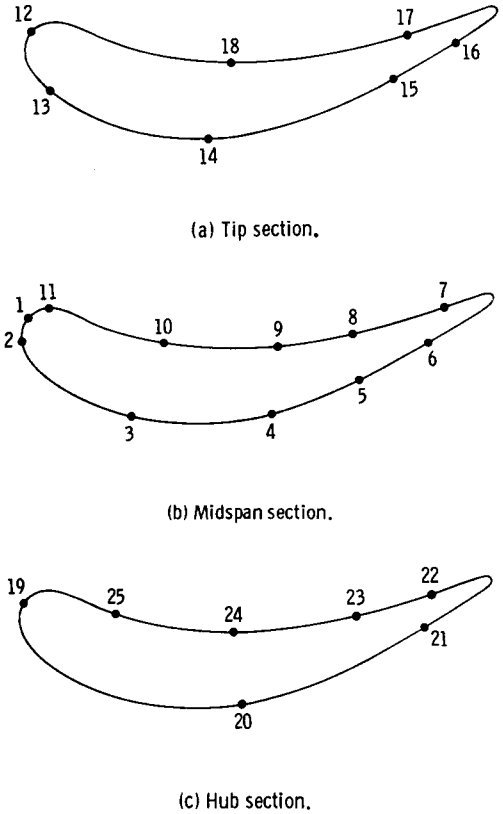


Figure 3. - Schematic showing thermocouple loactions on test vanes 2 and 3.

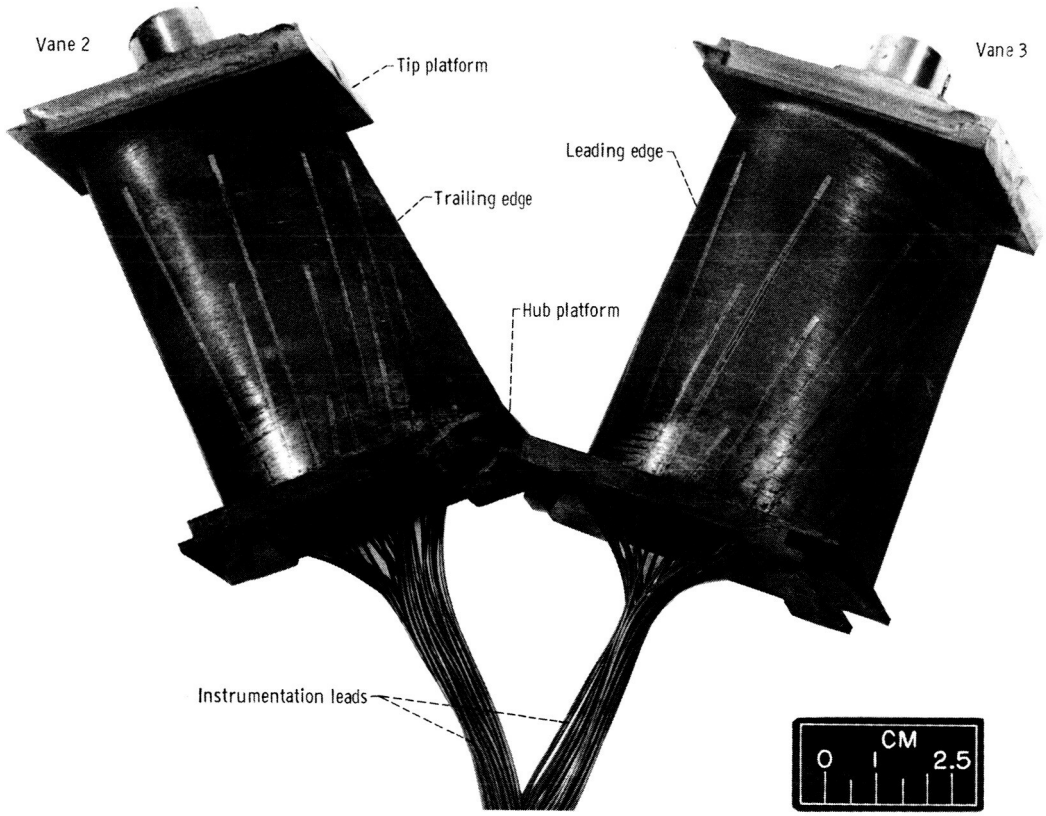


Figure 4. - Radiation correction test vanes showing suction surface.

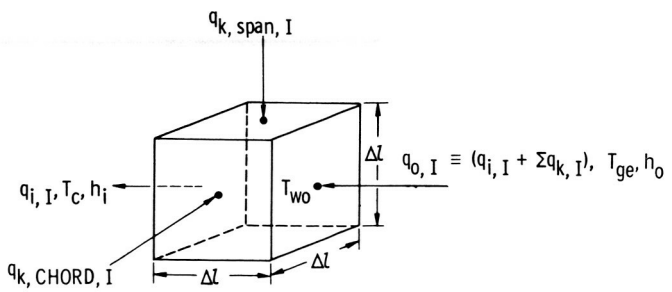


(a) Case I.

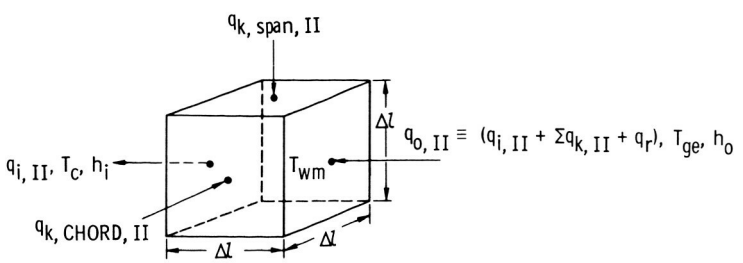


(b) Case II.

Figure 5. - Schematic of turbine vane airfoil element showing three-dimensional heat balance.

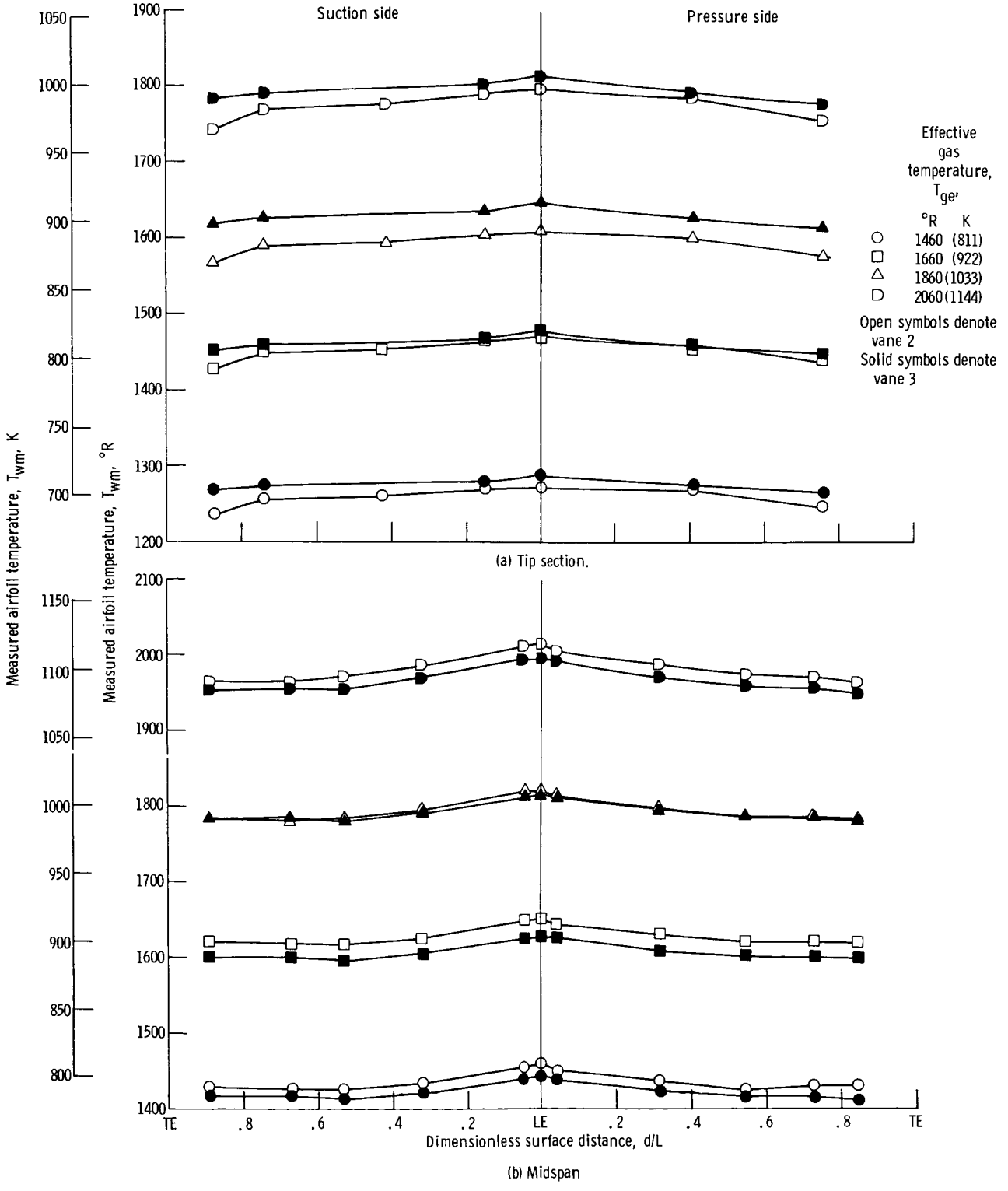


Figure 6. - Airfoil temperature distribution over range of gas stream temperature and without platform cooling.

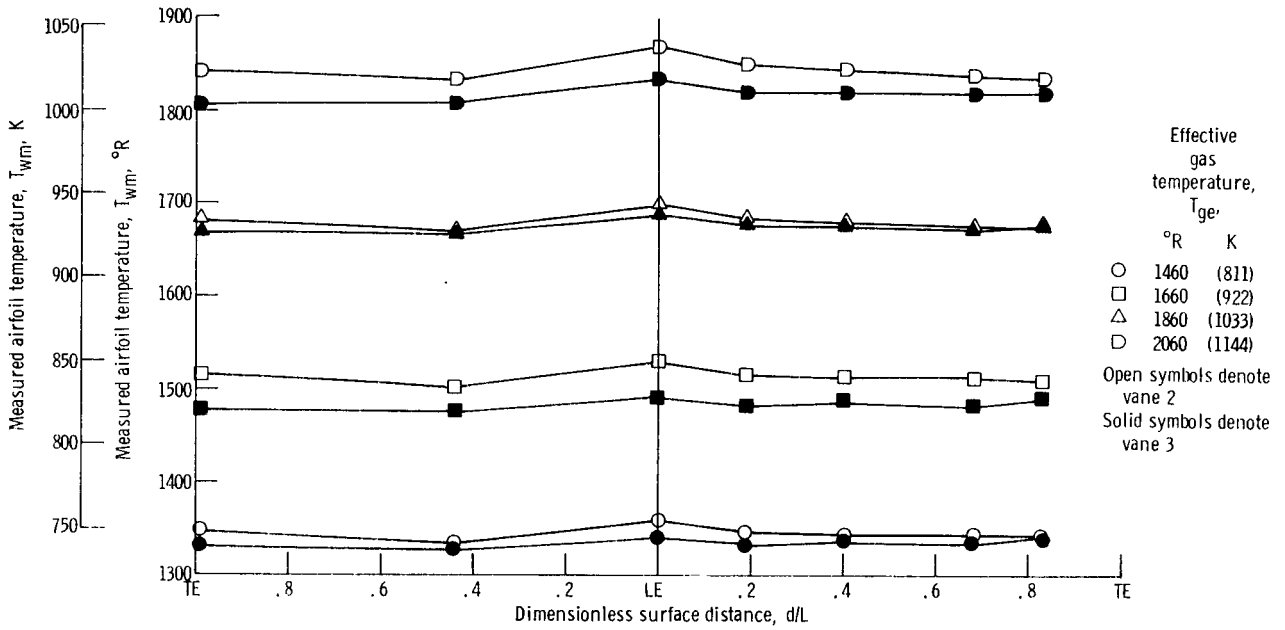


(c) Hub section.

Figure 6. - Concluded.

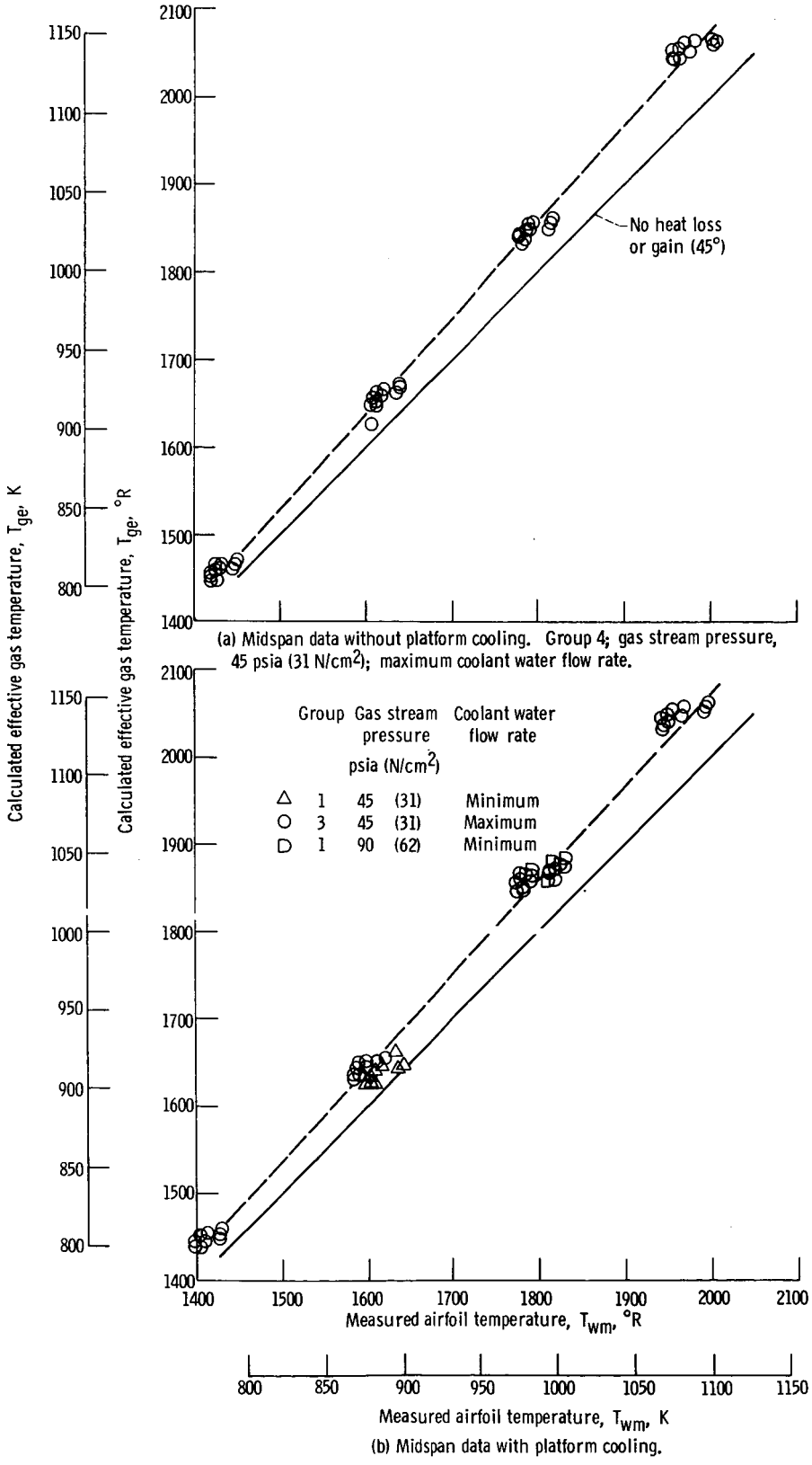


Figure 7. - Comparison of local effective gas temperatures and measured vane airfoil temperatures.

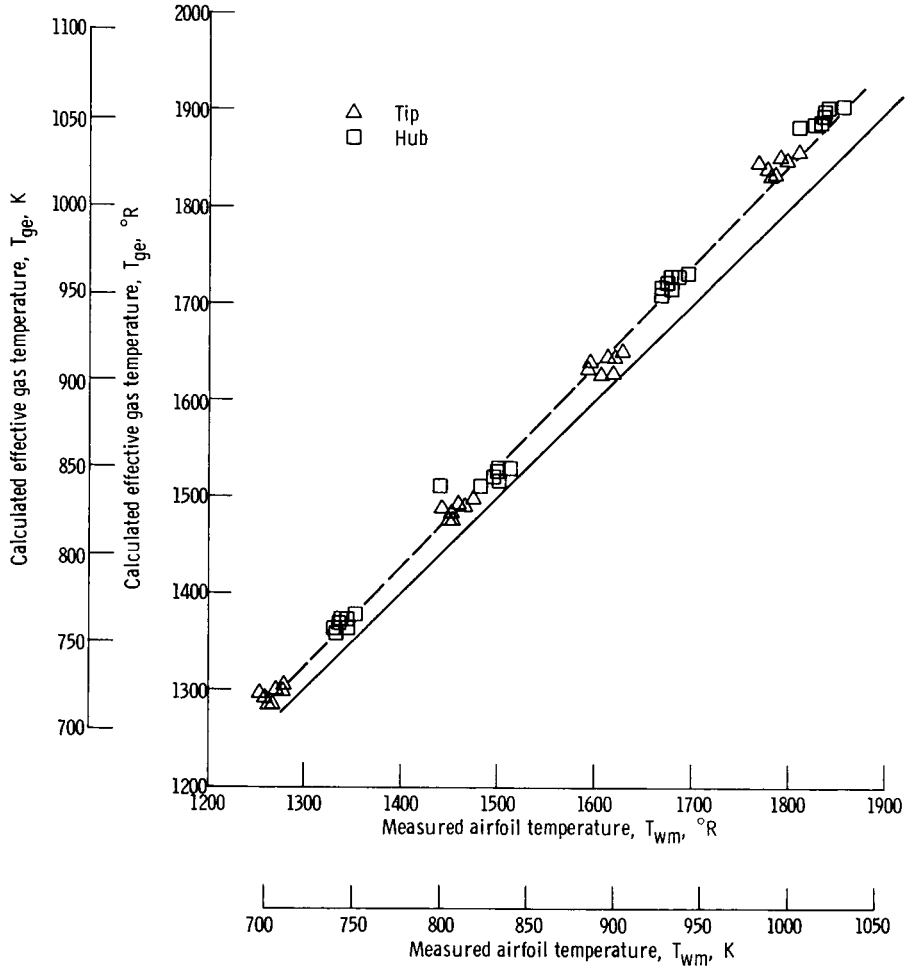


(c) Hub and tip data without platform cooling air. Group 4; gas stream pressure, 45 psia (31 N/cm$^2$); maximum coolant water flow rate.

Figure 7. - Concluded.

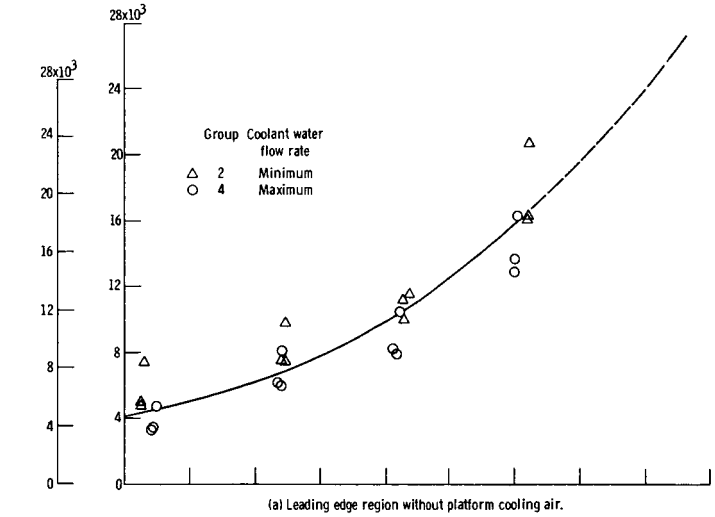


(a) Leading edge region without platform cooling air.

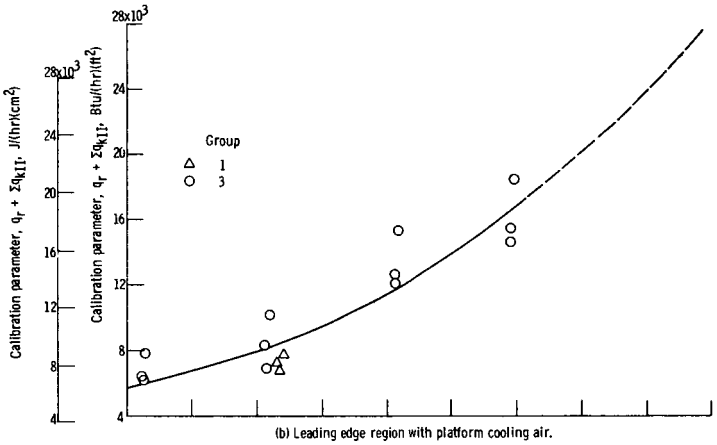


(b) Leading edge region with platform cooling air.

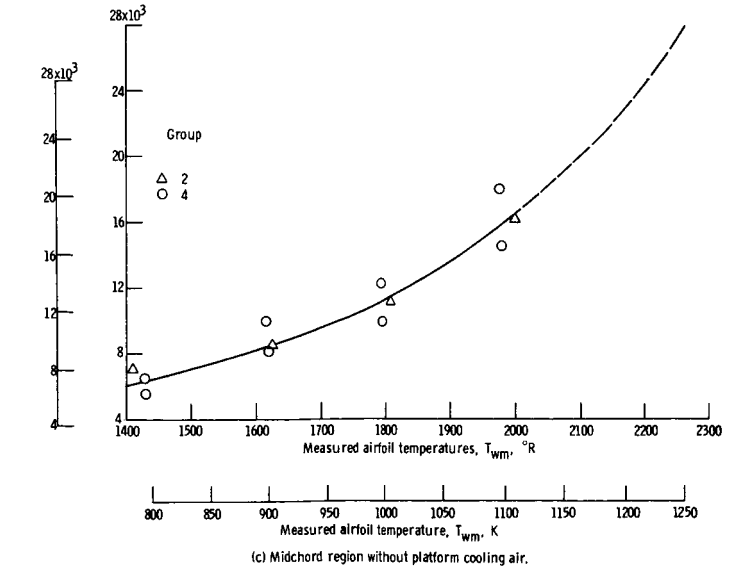


(c) Midchord region without platform cooling air.

Figure 8. - Variation of calibration parameter with vane airfoil temperature. Midspan; Gas stream pressure, 45 psia (31 N/cm$^2$).

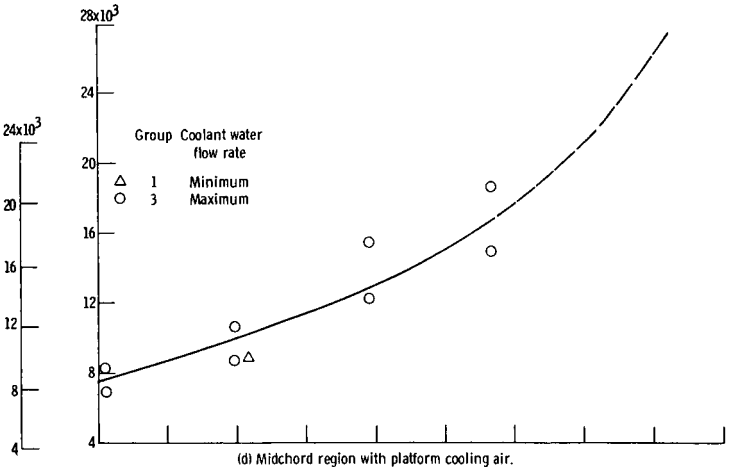


(d) Midchord region with platform cooling air.

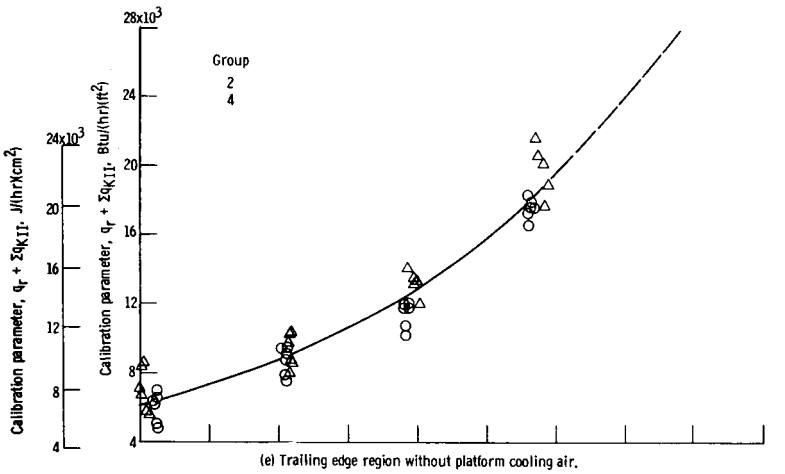


(e) Trailing edge region without platform cooling air.

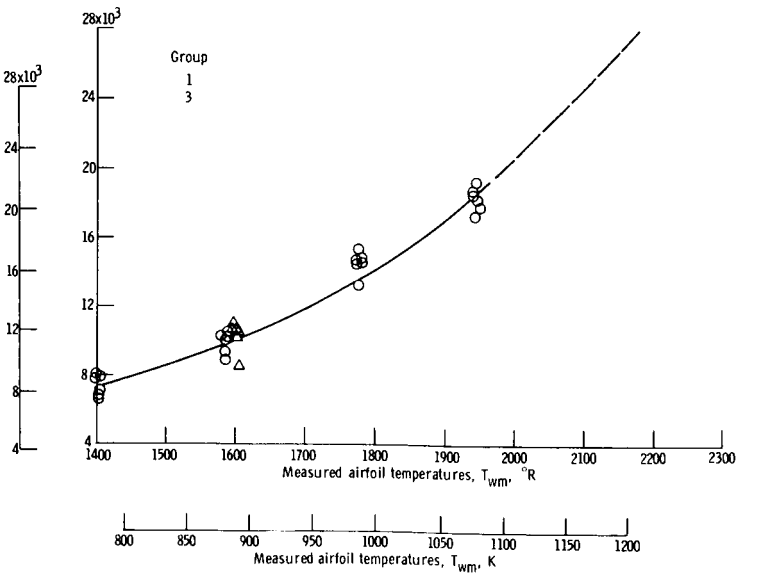


(f) Trailing edge region with platform cooling air.

Figure 8. - Concluded.

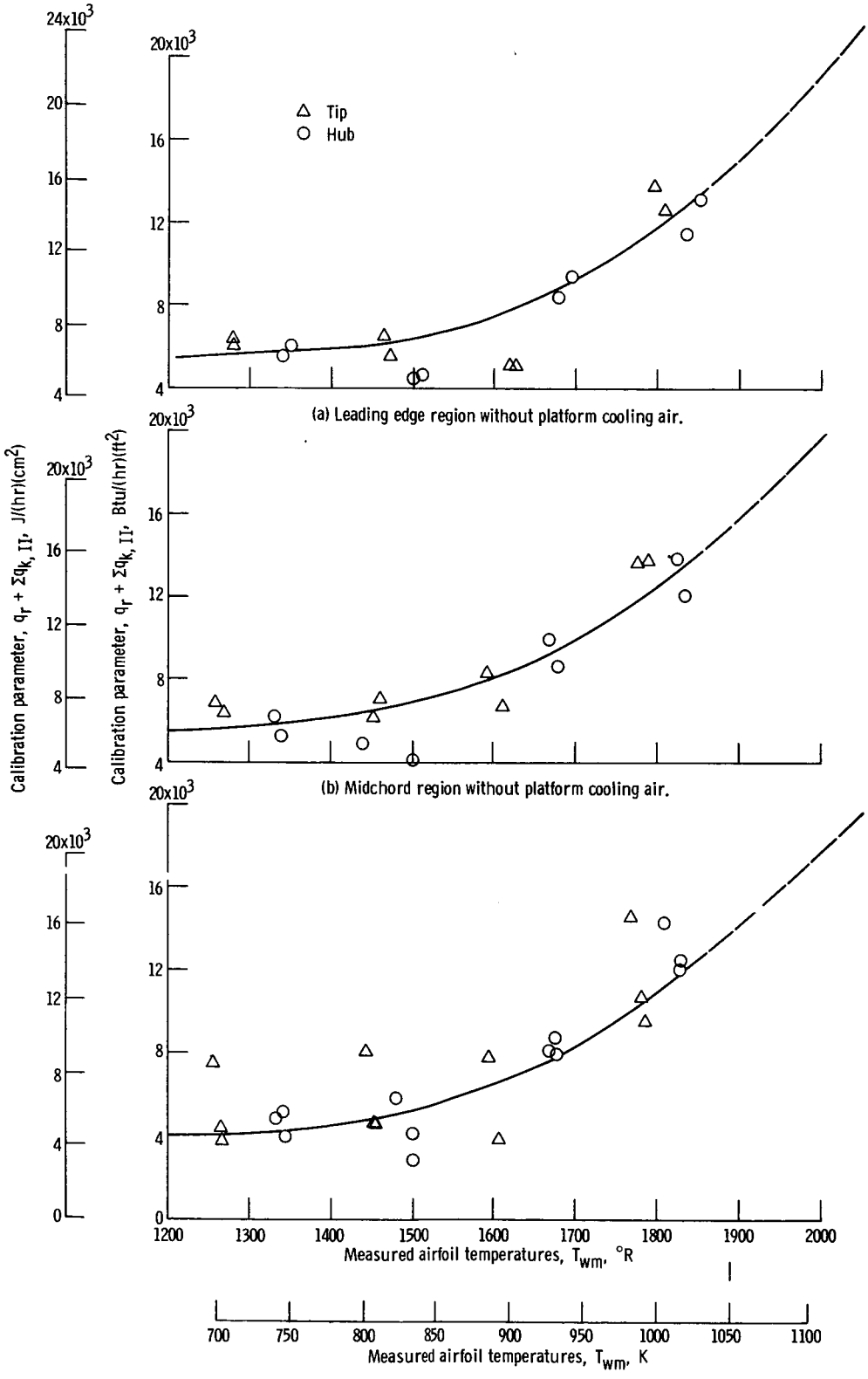


Figure 9. - Variation of calibration parameter with vane metal temperatures. Measurements taken at vane hub and tip. Group 4; gas stream pressure, 45 psia (31 N/cm$^2$); maximum coolant water flow rate.

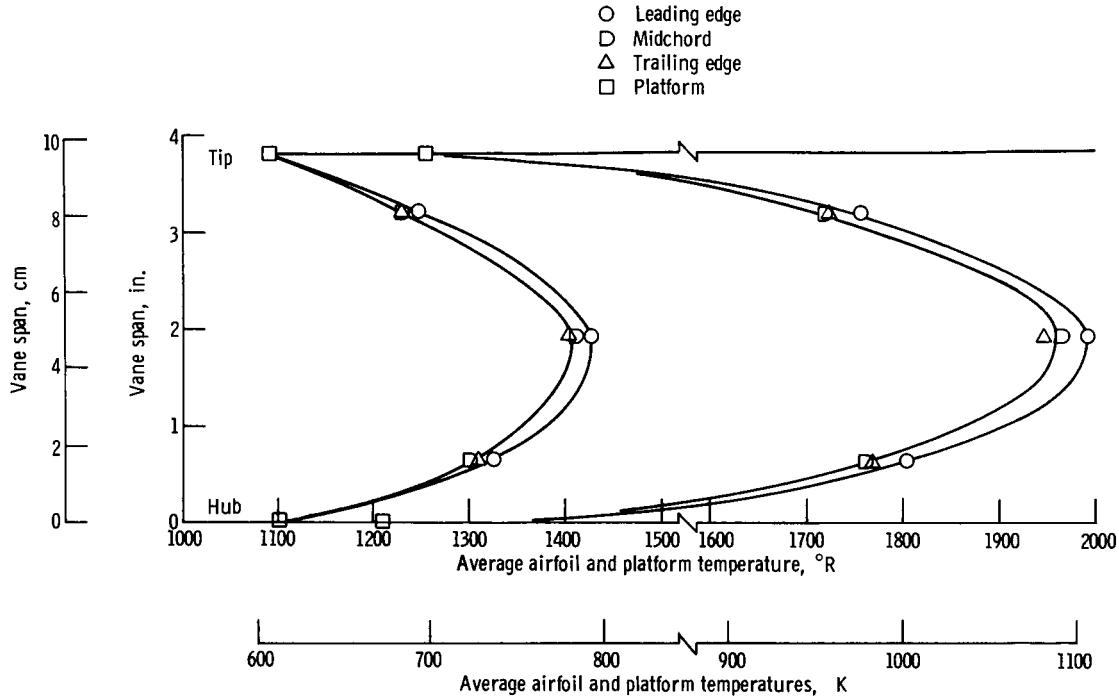


Figure 10. - Average spanwise temperature distribution in vanes 2 and 3. Separated between leading edge, midchord and trailing edge regions for nominal midspan total gas temperatures of 1460 R (811 K) and 2060 R (1144 K).

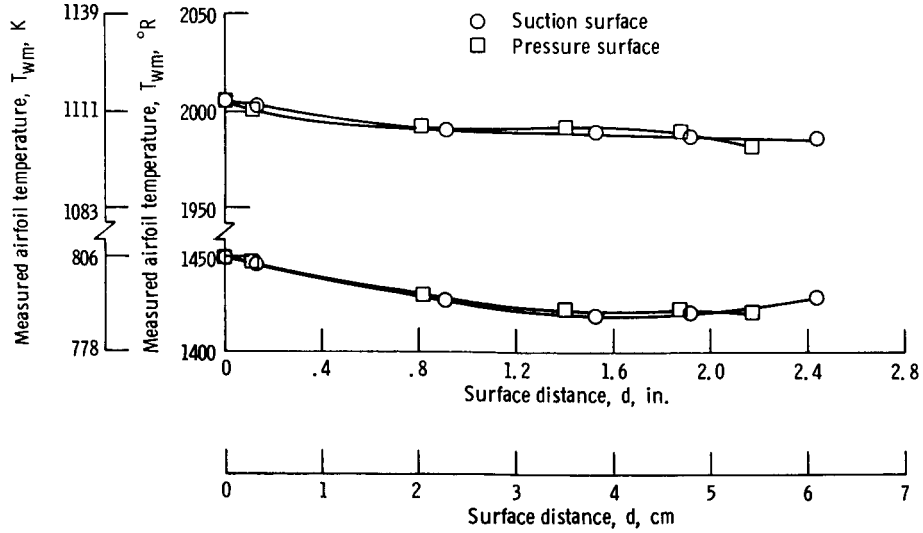


Figure 11. - Vane chordwise temperature profile for both suction and pressure surfaces. Nominal midspan gas temperature 1460° R (811 K) and 2060° R (1144 K).



NASA-Langley, 1971 — 33 E-5862